Adv. J. Sci. Eng.

Advanced Journal of Science and Engineering

https://adv-j-sci-eng.com

eISSN: 2717-0705

Original Research

Preparation and Characterization of Polypropylene/Organo-Muscovite Clay Nanocomposites by Melt Extrusion

Haydar U. Zaman[1,✉], Ruhul A. Khan[1]

[1]*Institute of Radiation and Polymer Technology, Bangladesh Atomic Energy Commission, Savar, Dhaka, Bangladesh*

✉*Corresponding Author*: H.U. Zaman; *Email*: haydarzaman07@gmail.com; *ORCID*: 0000-0002-1673-6915

Advanced Journal of Science and Engineering. 2022;3(1):23-34. https://doi.org/10.22034/advjse22031023

Received: 10 July 2021 / ***Revised***: 03 February 2022 / ***Accepted***: 07 February 2022 / ***Published***: 15 February 2022

Abstract: In this research work, polypropylene (PP)/organo-muscovite clay (OM) nanocomposites with different filler contents were manufactured using melt compounding technique in a twin-screw co-rotating extruder tracked by hot press method. Two compatibilizers such as maleated polypropylene and hexamethylenediamine modified maleated polypropylene copolymer were included in all nanocomposites containing 10 wt%. Mechanical properties have been observed to be influenced by OM nanoparticles as well as copolymer content. For tensile properties, the most observed were related to the sample with 5 wt% OM. The hexamethylenediamine modified maleated polypropylene copolymer system conferred superior tensile features than maleated polypropylene copolymer system and the PP/OM case. This outcome was confirmed from TEM and SEM micrographs. Evidently, the compatibilizers were operative to support the OM delamination. The hexamethylenediamine modified maleated polypropylene system had a partial exfoliation of PP/OM nanocomposites compared to the maleated polypropylene system. The inclusion of compatibilizers with OM has improved all tensile and thermal properties as well as the rheological behavior of nanocomposites, enhancing the strong interfacial interactions by compatibilizers.

Keywords: Polypropylene; Organo-muscovite clay; Nanocomposites; Compatibilizers; Mechanical properties.

Introduction

The common object of preparation and scientific research on the properties of polymer nanocomposites to create new polymer materials with increasingly advanced properties has increased over the last few years [1-4]. Polymer/organoclay nanocomposites have a high potential for industrial and academic applications, as they often reveal an extended range of mechanical, thermal, and other properties when compared with plain polymers or traditional micro and macro-composites [5]. One of the promises of maximum nanocomposites would be a hybrid based on organic polymers and inorganic clay minerals containing layered silicate [6]. The Toyota investigation team first tested polyamide-6/clay nanocomposites and discovered that the mechanical and thermal properties of the clay filler had developed at a considerably lower load

Copyright © 2022 to Advanced Journal of Science and Engineering as a Member of SciEng Publishing Group (SciEng)
This work is licensed under a Creative Commons Attribution 4.0 International License (CC-BY 4.0).

stage than traditional composites [7]. Polymer/clay nanocomposites were reported in the scientific literature [8-11]. López-Quintanilla et al. [12] report that three types of polymer/clay nanocomposites were commonly intercalated as a conventional nanocomposite, which allowed some parts of the polymer to be dispersed between layered silicate and exfoliated nanocomposites. Currently, PP/organoclay nanocomposites have attracted great research interest. PP is a thermoplastic engineering polymer, which has many necessary properties such as precision, dimensional durability, flame interruption, high thermal deformation temperature, and great impact strength, and expands their appeal. PP also enhances filling and is very suitable for mixing. However, the uniform dispersion of silicate layers in PP cannot be perceived due to the low polarity of traditional PP. In this case, nanotechnology will be used to more progress the features of PP. Polymers, such as kaolinite and montmorillonite (MMT), are the most widely used polymers in nanotechnology because of the swelling and layering of silicate nanocomposites with their ion-exchange properties. Other types of clay have the same potential as vermiculite and muscovite. Muscovite is the maximum level of charge concentration and uniform charge parceling and much cheaper than MMT. Nevertheless, PP/clay nanocomposites have become a more realistic possibility using compatibilizers such as functional oligomers. Such compatibilizers must have adequate polarity to communicate with the silicate layer and to blend bulk PP easily [13]. To improve the isolation of mineral clay in the PP matrix, investigators have generally used maleic anhydride (MA) [14, 15], which can develop the polarity of polymer molecules. PP/clay nanocomposites have used PPMA in most studies, as it has been able to provide the best degree of performance of all modified polyphenylene sulfide (PPS) investigated so far. In the present investigation, muscovite was organo-modified using cetyltrimethylammonium bromide (CTAB) as alkyl ammonium to produce organoclay (O-Muscovite, OM). In this study, we explored compatibilizers such as PPHMDA and PPMA in PP/OM nanocomposite. There is no such literature is available for the best knowledge of authors who discusses the effects of particular compatibilizers on the morphological, mechanical, thermal, and rheological properties of PP/PPHMDA/OM or PP/PPMA/OM nanocomposites using the blending procedure. The response of nanocomposites is then related to the effects of organic modifications on their dispersion, mechanical, thermal, and rheological behavior in several compatibilizers.

Materials and Methods

The thermoplastic polymer matrix PP was obtained from MTBE (Malaysia) Sdn. Bhd. as the pellets form with a specific gravity of 0.91-0.92 and a melting temperature of 160-170 °C. Uninspendable muscovites with an average size of about 20 micrometers were found from the Bidor Minerals (M) Sdn. Bhd. The modified muscovite, known as organomuscovite (OM), was prepared by the cation exchange of lithium nitrate ($LiNO_3$) and cetyltrimethylammonium bromide (CTAB), supplied by Sigma Aldrich (M) Sdn. Bhd. Poly(propylene-g-maleic anhydride) copolymer (PPMA) with 8-10 wt% maleic anhydride (MA) was acquired from Sigma Aldrich (M) Sdn. Bhd. Hexamethylenediamine was supplied by Sigma Aldrich with M_w = 116.21 g/mol; T_m = 42 °C; ρ = 840 kg/m^3 and water solubility = 490 g/l.

Arrangement of PP/OM Nanocomposites

PPMA was treated by HMDA (marked as PPHMDA) in xylene solution at 110 °C for one and a half h and then exhausted with distilled water, washed in hot water, and dried at 80 °C for 24 h. The PPHMDA preparation is illustrated in Scheme 1. Muscovite powder and $LiNO_3$ powder were

mechanically mixed with a ratio of 1:17. The mixture was then heated in a furnace at 250 °C for 12 h. The resulting product was soaked in 200 ml of distilled water and filtered, and then dried at 100 °C for 12 h. This product was obtained as silver powder and was labeled as Li-muscovite. The Li-muscovite was mixed with CTAB aqueous solution at room temperature. Then the mixtures were put in a hydrothermal reactor (100 ml) of Teflon lined stainless-steel autoclave and then heated at 180 °C for 12 h. After the reactions, all the surfactant-muscovite (organoclay) products were filtered and then washed three times with ethanol, dried in a vacuum oven at room temperature. The obtained CTA^+-muscovite samples were named organomuscovite (OM). The PPHMDA/OM nanocomposites were prepared by using organically modified muscovite clay mixed with a xylene solution and PPHMDA at 120 °C for 6 h. The PPHMDA/OM nanocomposites were then precipitated with an excess amount of deionized water, washed with hot water, and dried at 100 °C for 12 h in a vacuum. Before compounding, all the raw materials were dried in a vacuum oven at 80 °C to constant weight for a minimum of 12 h and then cooled down to room temperature. The nanocomposite samples were prepared with varying amounts of OM (3, 5, and 7 wt%), the preweighed quantity of PP with two types of compatibilizers (PPHMDA or PPMA) at a fixed amount of 10 wt% as follows. The compositions of the arranged nanocomposites are recorded in Table 1. Melt blending was performed with a co-rotating twin-screw extruder (Brabender Plasticorder, model: PLE-331). The screw speed and temperature profiles were set at 60 rpm and 160, 170, 200, 180 °C, respectively. The pellets of PP were tumble-mixed with OM with compatibilizers and antioxidants (Irganox-B225) in a sealed plastic bag. All ingredients were mixed at 25 °C for 6 min and immediately filled with a twin-screw extruder for blending. The mixing time for each sample was 10 min. The extruded samples were hot-pressed at 180 °C for 5 min under a pressure of 10 MPa and then cooled to 25 °C. The obtained specimen sheets were used for various measurements.

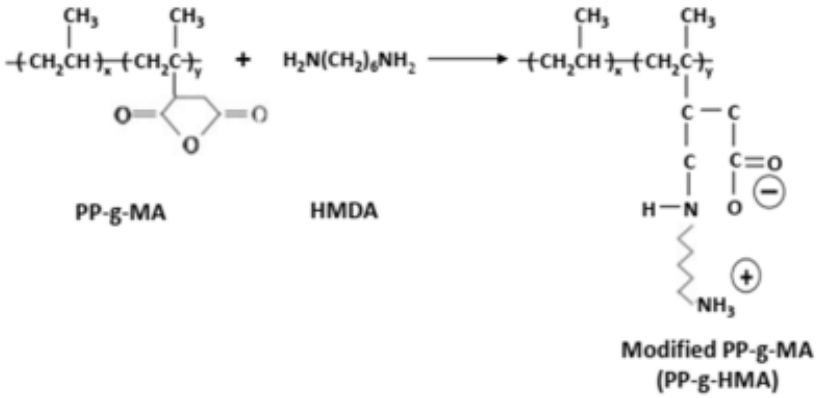

Scheme 1: A conceptual illustration of the preparation of PPHMDA.

Table 1: Compositions of nanocomposites.

Sample	Code	PP wt%	OM wt%	PP-g-HMDA wt%	PP-g-MA wt%
PP	PP	100	n/a	n/a	n/a
PP/OM3	M3	97	3	n/a	n/a
PP/OM5	M5	95	5	n/a	n/a
PP/OM7	M7	93	7	n/a	n/a
PP/PP-g-MA/OM5	M5M10	85	5	n/a	10
PP/PP-g-HMDA/OM5	M5HM10	85	5	10	n/a

Morphological Studies

Nanocomposite samples were performed by the transmission electron microscope (TEM; JEOL JEM-2010) with an accelerating voltage of 200 kV. Extruded samples were microtomed in the form of ultrathin pieces (about 100 nm thickness) by a microtome with a diamond knife (Leica Ultracut UCT) then the pieces were imaged in the TEM. Extruded samples were fractured in liquid nitrogen and the fracture surface of the samples was observed using Scanning Electron Microscope (SEM; JEOL, Japan JSM-6360LV) at an accelerating voltage of 15 kV. The fracture surfaces of the sample were covered with a tinny layer (10–20 nm) to protect the gold.

Bulk Tensile and Hardness Features Evaluation

Tensile features such as strength, modulus, and elongation at break were evaluated of the virgin PP, PP/OM, PP/PPMA/OM, and PP/PPHMDA/OM nanocomposites. Composite samples were performed according to ASTM standard method by a screw-driven universal testing machine (model: Instron 4466). The crosshead speed of 20 mm/min and the gauge length was 10 mm. Shore hardness tests of the composite samples was performed by the Japan Shore Hardness Testing Machine (Type D). The test was done according to the ASTM D790 standard. All the samples were conditioned at 25 °C and 55 % relative humidity. Five samples were tested in each case and the mean values were calculated.

Thermal Characterizations

The thermal fixity of the nanocomposites (weighed 8-10 mg) was measured by a thermogravimetric analyzer (TGA, TA instruments Q500) at a temperature of 20 °C/min under N_2 atmosphere. The heat distortion temperature (HDT) of PP and its nanocomposite was determined by ASTM D 648 using $125 \times 12.50 \times 3.0$ mm^3 dimensional specimens. The test was performed using Advanced HDT/Vicat softening point apparatus (Ray Ryan Test Equipment, Ltd) with a heating rate of 2 °C/min. The melting and crystallization temperatures and the crystallinity of the samples were performed by Differential Scanning Calorimetry (Perkin Elmer DSC-7, Wellesley, MA, USA) at a heating rate of 10 °C/min in the N_2 environment. The weight of the sample was between 5-8 mg. The percentage crystallinity (X_c) was calculated by the following equation: X_c (%) = ($\Delta H_m/\Delta H_f$) $\times$ 100; where ΔH_m is the melting enthalpy of semicrystalline PP and ΔH_f is the heat fusion of crystalline PP.

Rheological Measurements

Rheological features of the nanocomposites were performed by a Paar Physica UDS apparatus. To make a disc sample, nanocomposites were compression molded using a hot press at 220 °C and a frequency range of 0.1-100 rad/s.

Results and Discussion

The Dispersity of Organo-Muscovite Clay; TEM Observation

Figure 1 depicts TEM photomicrographs of PP/OM nanocomposites consisting of 5 wt% OM (designated as M5) and 10 wt% PPMA (denoted as M10) or 10 wt% PPHMDA (marked as HM10). Figure 1 (a) displays considerably bigger OM elements, which are not intercalated and probably form a ‘micro composite’ structure, possibly due to the absence of PPMA or PPHMDA. The black shape (piled silicate platelets) exhibits the OM tactoids and the rest of the region represents an uninterrupted PP. Nevertheless, some black shapes may indicate some weakly dispersed OM

aggregates. Figure 1 (b) on the other hand shows relatively small OM elements compared to Figure 1 (a) and the OM elements were separated into lighter parts by the blending manner. Anyway, a better dispersion can be acquired after the addition of PPHMDA as a compatibilizer, which performances as an intercalator between PP and OM (Figure 1, c). PPHMDA systems have better and more uniform dispersion of OM in the PP matrix than in the PPMA system because of less black shape in that for PPHMDA. Therefore, compatibilizers should be mixed with OM and matrixes to better disperse OM in the matrix and to increase the tensile features.

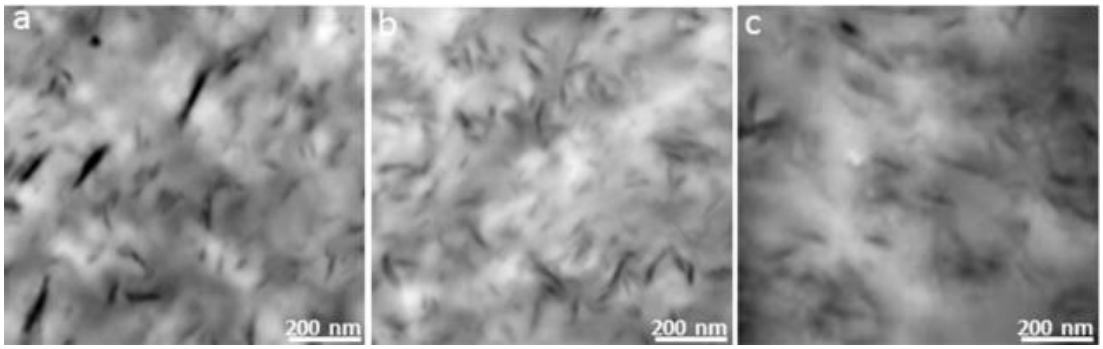

Figure 1: Tensile TEM micrograph of **(a)** M5, **(b)** M5M10, and **(c)** M5HM10 nanocomposite.

SEM Analysis

Figure 2 (a), (b), and (c) represent the SEM photomicrographs of PP/M5, PP/M5M10, and PP/M5HM10 nanocomposites, respectively. The particles of OM in Figure 2(a) were randomly distributed in the PP matrix and some large portions were exposed above the fracture surface. Big elements are distributed in PP to PP/OM nanocomposite so that no functional polymer is present and the interfaces appear to be individually wet and/or weak to the adhesion of the components. The presence of PPMA or PPHMDA changes the morphology. The PP/M5M10 system had some large parts and the average particle size was smaller than the PP/M5 system. As shown in Figure 2(c), the PP/M5HM10 system was more uniformly dispersed in the PP matrix than the PP/M5M10 system. Changes in both particle size and interface indicate that PPMA or PPHMDA help break down particles and modify interfacial interactions. This result agrees with the outcomes of the tensile features in Figure 4.

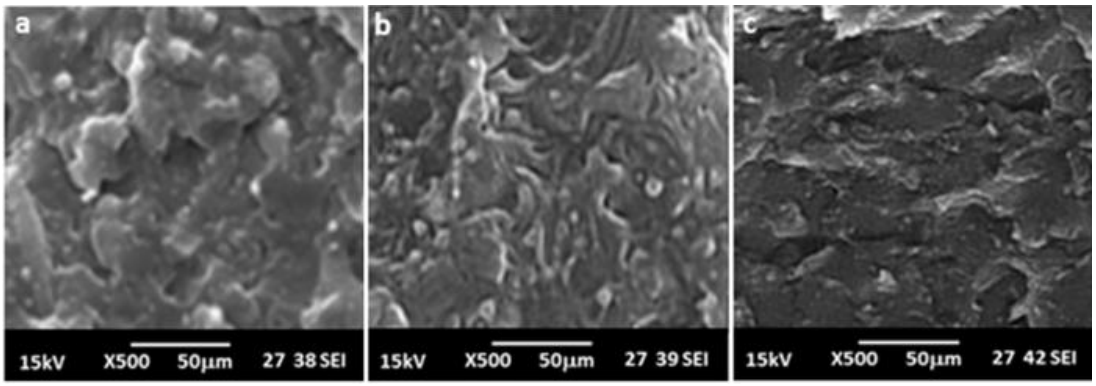

Figure 2: SEM photomicrographs of **(a)** M5, **(b)** M5M10, and **(c)** M5HM10 nanocomposites.

Effect of OM Loadings

Typically, the tensile features (tensile strength, TS; tensile modulus, TM; and elongation at break, Eb (%)) of immiscible mixtures without compatibility are weak due to weak interfacial bonds

between the components. Tensile features were measured in virgin PP and its nanocomposites with OM content ranging from 3 to 7 wt %. Variations of TS and TM of nanocomposites against OM content are expressed in Figure 3(a). The value of TS and TM increased with increasing OM content up to 5 wt% due to the enhancing impact of OM with higher proportions and then decreased. The TS and TM of the virgin PP were approximately 32.5 MPa and 1158 MPa, respectively, corresponding to the zero OM content in the Figure. It showed that TS increased significantly by 15.6 % and TM by 17.8 % during the use of 5 wt% OM and delivered a good strengthening impact. Further increase in OM loading weakens the strengthening impact and makes it unable to transfer stress proficiently. Elongation at break is too a significant tensile feature for ingredients of this class. Usually, the inclusion of OM in polymeric components decreases the elongation at break. The outcomes of elongation at break (%) are displayed in Figure 3 (b). The value of elongation at break has decreased significantly with the increase in OM content.

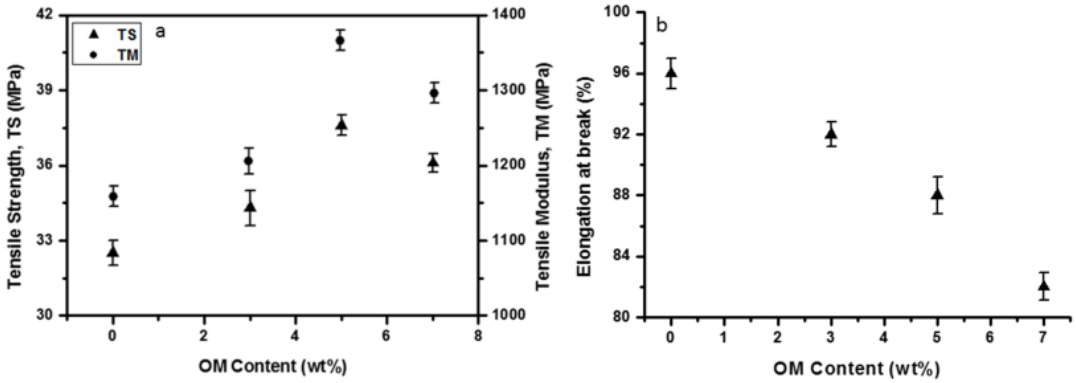

Figure 3: (a) Tensile strength and tensile modulus and **(b)** elongation at break (%) of virgin PP and its nanocomposites.

Tensile Features of Prepared Nanocomposites

The results of TS, Eb (%), and TM of PP/OM nanocomposites are displayed in Figures 4 (a) and 4 (b), respectively. Tensile features of virgin PP and PP/OM were loaded with OM at the prescribed amount of 5 wt% and were kept at 10 wt% in the presence of compatibilizers. As in Figure 4 (a), the TS of virgin PP was approximately 32.5 MPa and the relevant value of 5 wt% OM load for nanocomposite was raised to 37.6 MPa, an increase of 17 % over PP. Increased TS may be due to the long aliphatic chain in OM leading to a rich interfacial bond between the matrix and the OM. The TS of PP/M5HM10 was approximately 42.3 $\pm$ 0.8 MPa, which was higher than that of PP and higher than that of PP/M5M10 (39.8 $\pm$ 0.5 MPa). The increased TS of the compatibilized system is expressed by the good distribution produced by the compatibilizer and by an enhanced solid-state adhesion, which can transfer more stress from the matrix to the dispersion stage. These outcomes are compatible with the results of research studies conducted by Chen et al. [16]. As previously described in TEM, dispersed compatibilizers can also modify matrix features to contribute to the observation of the tensile features of nanocomposites. Thus, M5M10 was applied less TS than M5HM10 within the interphase. These results are consistent with Szazdi et al's pioneering hypothesis that PP/OM nanocomposites used as PP-g-MA could not guarantee higher TS for layered silicate nanocomposites [17]. As shown in Figure 4 (b), the TM of virgin PP was approximately 1158 $\pm$ 45.3 MPa, and the relevant value of 5 wt% OM load for nanocomposite was raised to 1365 $\pm$ 51.2 MPa, an increase of 18 % over PP. Increased stiffness may be responsible for the dispersion of OM which can stabilize the polymer phases which leads to stiffness [18]. Also, the TM of the M5HM10

nanocomposite (1619 ± 48.6 MPa) increased by 9 % over that of the M5M10 nanocomposite (1483 ± 53.5 MPa). As shown in Figure 4 (a), the elongation at break was declined for all nanocomposites of the same OM and M5M10/M5HM10 materials compared to PP. In principle, the introduction of mechanical restraint reduces the matrix distortion as the cause of the filler.

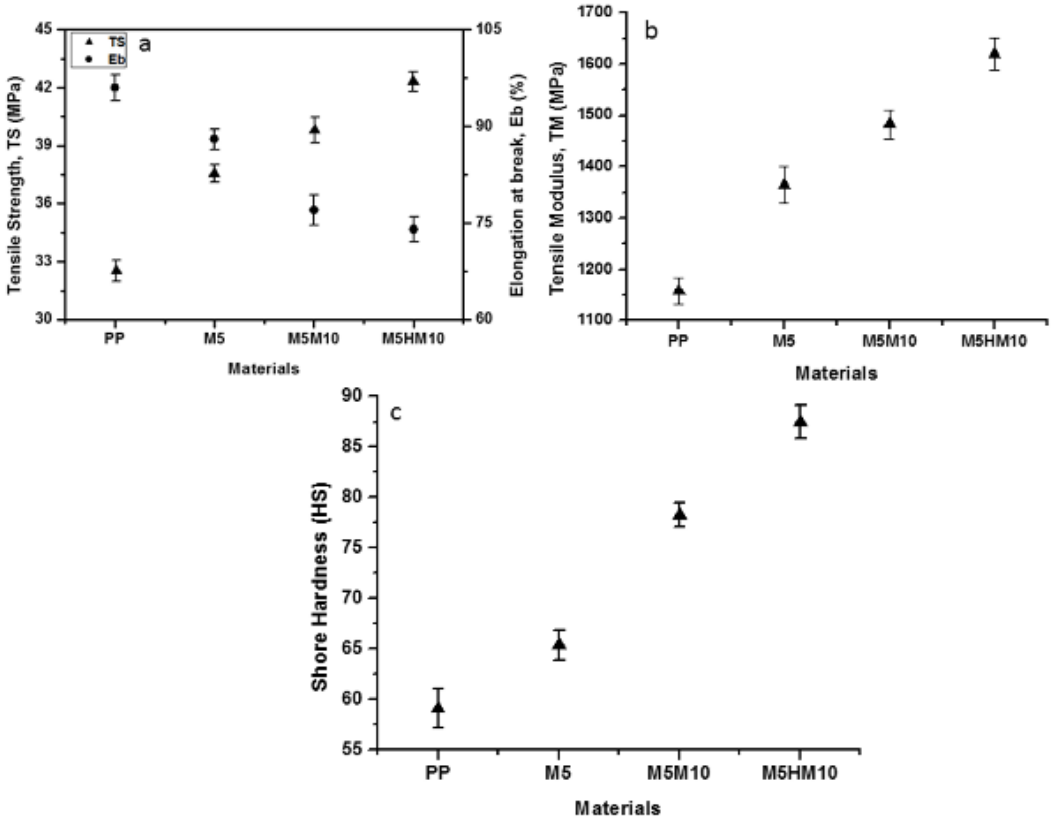

Figure 4: (a) Tensile strength and elongation at break (%); **(b)** tensile modulus, and **(c)** hardness features of virgin PP and its nanocomposites.

Hardness Property Studies

The hardness of virgin PP and its nanocomposites are displayed in Figure 4 (c). As shown in Figure 4 (c), the hardness of virgin PP was approximately 59.1 Hs, and the relevant value of 5 wt% OM load for nanocomposite was raised to 65.4 Hs, an increase of 11 % over PP. This may be due to the presence of intercalated/exfoliated OM platelets in the PP matrix. The inclusion of M5M10 and M5HM10 in the PP improved the surface hardness to 78.3 Hs for the M5M10 and 87.5 Hs for the M5HM10. This is mainly attributed to the reinforcing effect of M5M10 or M5HM10. Thus, the integration of OM and two types of compatibilizers in PP must alter the surface features of nanocomposite components based on the surface tensile feature observation.

Thermal Properties of PP and its Nanocomposites; Thermal Stability

The TGA thermograms of virgin PP and its nanocomposites are shown in Figure 5 (a). The decomposition temperatures of virgin PP and its nanocomposites are listed in Table 2. For example, taking the initial decomposition temperature (T_{onset}), Figure 5 (a), and Table 2 display that the T_{onset} increased from 333.4 °C for virgin PP to 349.1 °C for M5 system with a char residue of 20.9 wt%, indicating that the thermal stability of PP was developed. For the M5M10 system, the T_{onset} of the nanocomposite was about 19.8 °C better than that of the PP. There were two possible explanations, one was that the intercalating effect of the M5M10 system resulted in better distribution of OM in

PP and a further increase in thermal stability for PP, the other was that the M5M10 system itself increased thermal stability. For the M5HM10 system, the T_{onset} increased from 333.4 °C in virgin PP to 369.2°C. The introduction of the M5HM10 system further enhanced the thermal stability of PP because the T_{onset} of M5M10 had a higher char residue of about 34.9 wt%, which displays that the distribution state of OM in the matrix played a vital role in thermal properties. As expected, both $T_{25\%}$ and $T_{60\%}$ for the M5M10 and M5HM10 were 10.2, 21.3, 11.1, and 39.1 °C higher than the M5. One possible reason for this is that M5M10 or M5HM10 had a higher $T_{60\%}$ than M5, which helped to develop the thermal stability of nanocomposites. Other factors were perhaps the intercalated impact of M5M10 or M5HM10 and the fine distribution of OM in the PP matrix.

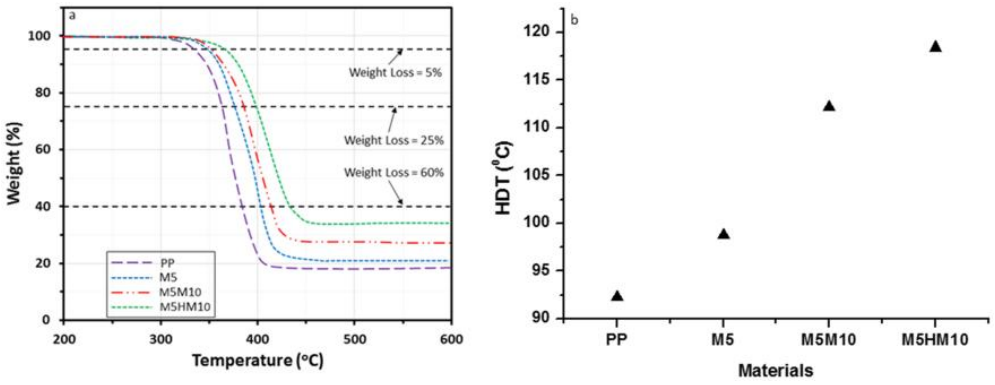

Figure 5: (a) TGA curves, and **(b)** heat distortion temperature of virgin PP and its nanocomposites.

Table 2: Thermal degradation temperatures of virgin PP and its nanocomposites.*

Sample	T_{onset} (°C)	$T_{25\%}$ (°C)	$T_{60\%}$ (°C)	Char residue at 600 °C (wt%)
PP	333.4	364.9	386.2	18.1
M5	349.1	378.6	404.7	20.9
M5M10	353.2	388.8	415.8	27.8
M5HM10	369.2	399.9	434.8	34.9

*T_{onset}: initial decomposition temperature at which 5 % weight loss occurred; $T_{25\%}$: the temperature at which 25 % weight loss occurs; $T_{60\%}$: the temperature at which 60% weight loss occurs.

Heat Distortion Temperature (HDT)

Figure 5 (b) shows the thermal behavior, measured as HDT, of virgin PP and its nanocomposites. The HDT of the M5 system was about 6.5 °C greater than that of the virgin PP, indicating that the thermal stability of the PP was developed. This agrees with the previously discussed TEM results. The existence of strong hydrogen bonds between PP and OM surfaces can be attributed to the improvement of HDT, it is responsible for better mechanical stability of nanocomposite and not an increase in melting temperature, which was unforgettable in nanocomposite compared to virgin PP. Compared to the M5 system, the M5M10 system shows better enhancement in HDT due to better distribution and exfoliation of OM in the PP matrix. Furthermore, the M5HM10 system exhibits the maximum HDT values. A more advanced exfoliated structure can be recognized in the M5HM10 system as confirmed by the previously discussed TEM results.

DSC Measurements

The outcomes of crystalline and melting peak temperatures of virgin PP, M5, M5M10, and M5HM10 nanocomposites are demonstrated in Figures 6 (a) and 6 (b), respectively. As shown in Figure 6 (a),

the T_c of the virgin PP was approximately 111.6 °C and indicates the compatibilizer that plays the nucleating role of enhanced Tc for the M5M10 or M5HM10 system. The Tc of PP was slightly increased to 113.2 °C for the M5 system. The impact of Tc growth on the existence of OM can be clarified by the probability of the performance of OM as an effective nucleating agent of the PP matrix. For the M5M10 system, Tc has been increased to 116.3 °C, indicating the nucleation impact of M5M10 for the PP matrix. It is fascinating to note that the Tc of M5HM10 improved to 118.7 °C, much larger than the PP and larger than the M5M10 system. Thus, the PP crystallization process exaggerates the impacts on the compatibilizer and OM, possibly increasing the PP molten viscosity of the OM, increasing the local shear stress, and making the compatibilizer of M5HM10 a more uniform network. Moreover, the Tm of PP was somewhat affected by the inclusion of OM and/or compatibilizers due to persuaded defective crystalline (Figure 6 (b)). No isolating impact was found from both compatibilizers, suggesting that the compatibilizers associated with the structure of PP and the crystal formation were not affected. The degree of crystallinity (X_c, %) of virgin PP and its nanocomposites are demonstrated in Figure 6 (c). OM has an unremarkable impact on X_c (%), while the compatibilizer induces great growth of X_c (%) for M5M10 and M5HM10 systems. To consider the nucleation impact of the compatibilizer on PP, one can assume that the crystallinity of the PP in M5HM10 is mostly ascertained by the compatibilizer rather than that of M5M10. Since the overhead outcomes were very naturally attractive, OM was deliberated as an active nucleating deputations due to its superior surface area when exfoliated. Nevertheless, due to the impacts of welding, plasticizing, and/or defects noted, the interface nucleation efficiency is impaired. Specifically, the great nucleating efficacy of OM was hampered by a high proportion of compatibilizers [19].

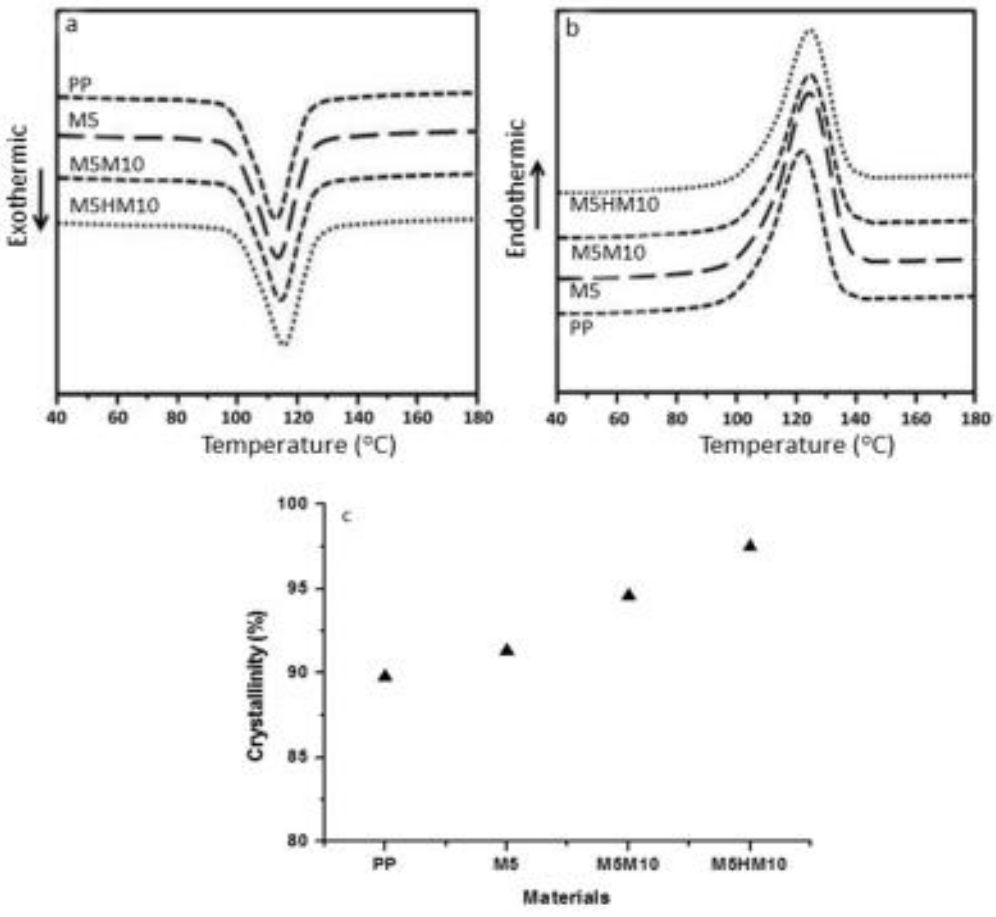

Figure 6: DSC of **(a)** crystallization thermograms, **(b)** heating thermograms, and **(c)** crystallinity of virgin PP and its nanocomposites.

Rheological Measurements

Figure 7 (a) - (c) provides the storage modulus (G'), loss modulus (G"), and complex viscosity (η*) of the virgin PP, M5, M5M10, and M5HM10 systems as a function of the frequency, respectively. The G', G", and η* of the PP were increased by employing OM. This makes sense that M5HM10 has the maximum range of frequency studies in G' and G" (Figure 7 (a) and (b)). Expressly, in the low-frequency state, it was perceived that the G' and G" frequencies became distinct for M5HM10 and M5M10, which are the distinctive behavior of hard-core components. The increases of G' and G" at lower frequencies indicate a stronger interaction between OM and PP. This conduct and tendency to increase G' and G" in the low-frequency region will be featured below to determine the extent of OM. The values of G' and G" are 4.9, 12.1, 30.2, 20.1 Pa and 98.3, 158.4, 230.6, 350.6 Pa for PP, M5, M5HM10, and M5M10 at frequencies of 10^{-1} rad/s, respectively. The outcomes indirectly displayed no interaction between the OM and PP chains and the OM could not demonstrate substantial filler impact deprived of any compatibilizer. Thus, the M5 system has been identified as a "macro-composite". On the contrary, considering the growth of G' and G", it has been confirmed that M5M10 produces considerable interaction between OM and PP, yet it is less than M5HM10 in a certain OM content. Expected OM will display better distribution in the M5HM10 system than the M5M10 system for the particular specimen formation. Figure 7 (c) demonstrates the complex viscosity (η*) versus frequency for virgin PP, M5, M5M10, and M5HM10 systems achieved from the frequency sweep exam. The η* declines with increasing frequency and indicates "non-Newtonian behavior". The influence of compatibilizers on η* was further frequent at lower frequencies than at higher frequencies, and with the addition of compatibilizers, this influence declines with increasing frequency due to the shear-thin behavior of nanocomposites. It was observed that M5M10 produces considerable interaction between OM and PP, yet it is less than M5HM10 in a certain OM content. This enrichment influence was intimately related to the large growth in the G' or G".

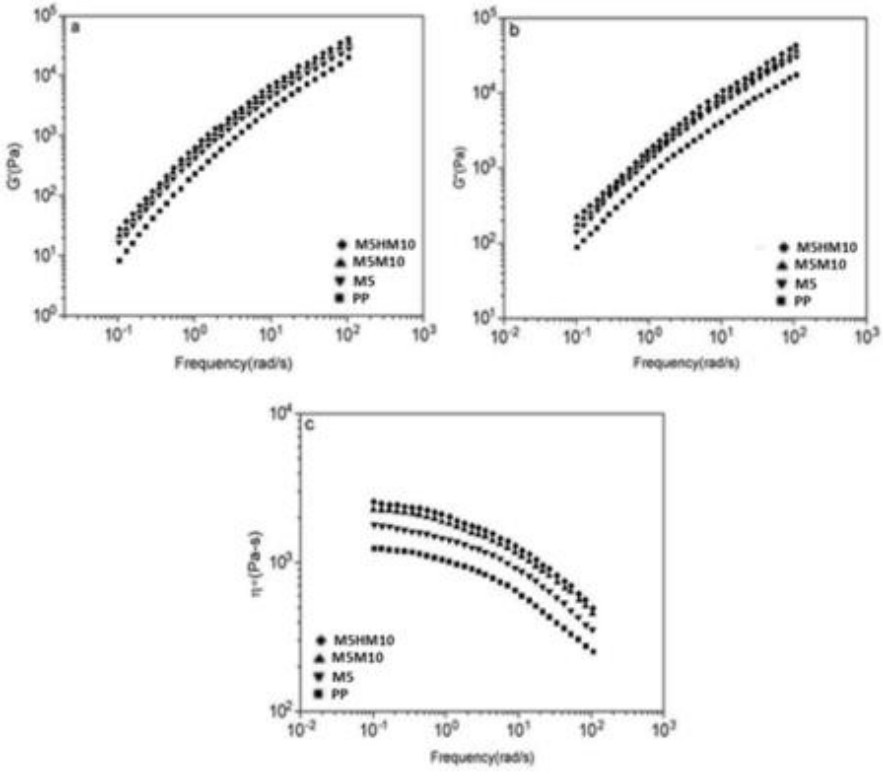

Figure 7: Virgin PP, M5, M5M10, and M5HM10 nanocomposites of (a) G', (b) G", and (c) η* as a function of the frequency.

Conclusion

PP/OM nanocomposites were prepared from a mixture of different OM contents and a certain content of PPMA or PPHMDA as a compatibilizer. Outcomes have shown that the inclusion of OM progresses tensile features. PPHMDA systems offer superior tensile and hardness features than PPMA systems and M5 systems. The morphological features of the outcomes exhibit that compatibilizers were operative to support the OM delamination. The PPHMDA system had a partial exfoliation of PP/OM nanocomposites compared to the PPMA system. The rheological features of the specimen also confirmed this outcome. TGA thermograms showed that the thermal stability of PP increased after the inclusion of M5M10 or M5HM10. The thermal steadiness of the specimens was observed in the order of M5HM10 > M5M10 > M5 > PP. HDT's outcomes observed that the M5M10 and M5HM10 systems were better than the OM systems. The DSC outcomes exhibited that the crystalline peak temperature of virgin PP was hardly influenced in nanocomposites.

Disclosure Statement

The author(s) did not report any potential conflict of interest.

References

1. Pesetskii S, Bogdanovich S, Aderikha V. Polymer/clay nanocomposites produced by dispersing layered silicates in thermoplastic melts. Research Anthology on Synthesis, Characterization, and Applications of Nanomaterials, IGI Global. 2021:1002-30.
2. Zaman HU, Khan RA. Comparing effects of different nanoparticles and compatibilizers on the properties of thermoplastic polyester elastomer nanocomposites. Advanced Journal of Science and Engineering. 2021;2:86-92.
3. Wen X, Min J, Tan H, Gao D, Chen X, Szymańska K, Zielińska B, Mijowska E, Tang T. Reactive construction of catalytic carbonization system in PP/C60/Ni(OH)2 nanocomposites for simultaneously improving thermal stability, flame retardancy and mechanical properties. Composites Part A: Applied Science and Manufacturing. 2020;129:105722.
4. Zaman HU, Khan RA. Effect of surface modified nano-calcium carbonate on the properties of polyethylene/nano-CaCO3 nanocomposites. International Journal of Research. 2021;8:212-22.
5. Zaman HU, Hun PD, Khan RA, Yoon K-B. Comparison of effect of surface-modified micro-/nano-mineral fillers filling in the polypropylene matrix. Journal of Thermoplastic Composite Materials. 2013;26:1100-13.
6. Yuan W, Guo M, Miao Z, Liu Y. Influence of maleic anhydride grafted polypropylene on the dispersion of clay in polypropylene/clay nanocomposites. Polymer Journal. 2010;42:745-51.
7. Hammami I, Hammami H, Soulestin J, Arous M, Kallel A. Thermal and dielectric behavior of polyamide-6/clay nanocomposites. Materials Chemistry and Physics. 2019;232:99-108.
8. Kodali D, Uddin M-J, Moura EA, Rangari VK. Mechanical and thermal properties of modified Georgian and Brazilian clay infused biobased epoxy nanocomposites. Materials Chemistry and Physics. 2021;257:123821.
9. Zaman HU, Hun PD, Khan RA, Yoon K-B. Polypropylene/clay nanocomposites: Effect of compatibilizers on the morphology, mechanical properties and crystallization behaviors. Journal of Thermoplastic Composite Materials. 2014;27:338-49.
10. Tan H, Wang L, Wen X, Deng L, Mijowska E, Tang T. Insight into the influence of polymer topological structure on the exfoliation of clay in polystyrene matrix via annealing process. Applied Clay Science. 2020;194:105708.
11. Papadopoulos L, Terzopoulou Z, Vlachopoulos A, Klonos PA, Kyritsis A, Tzetzis D, Papageorgiou GZ, Bikiaris D. Synthesis and characterization of novel polymer/clay nanocomposites based on poly (butylene 2, 5-furan dicarboxylate). Applied Clay Science. 2020;190:105588.

12. López-Quintanilla M, Sánchez-Valdés S, Ramos de Valle L, Medellín-Rodríguez F. Effect of some compatibilizing agents on clay dispersion of polypropylene-clay nanocomposites. Journal of Applied Polymer Science. 2006;100:4748-56.
13. Casalini T, Rossi F, Santoro M, Perale G. Structural characterization of poly-l-lactic acid (PLLA) and poly (glycolic acid)(PGA) oligomers. International Journal of Molecular Sciences. 2011;12:3857-70.
14. Bunekar N, Tsai T-Y, Huang J-Y, Chen S-J. Investigation of thermal, mechanical and gas barrier properties of polypropylene-modified clay nanocomposites by micro-compounding process. Journal of the Taiwan Institute of Chemical Engineers. 2018;88:252-60.
15. Wu M-H, Wang C-C, Chen C-Y. Preparation of high melt strength polypropylene by addition of an ionically modified polypropylene. Polymer. 2020;202:122743.
16. Chen WC, Lai SM, Chen CM. Preparation and properties of styrene-ethylene-butylene-styrene block copolymer/clay nanocomposites: I. Effect of clay content and compatibilizer types. Polymer International. 2008;57:515-22.
17. Százdi L, Pukánszky Jr B, Vancso GJ, Pukánszky B. Quantitative estimation of the reinforcing effect of layered silicates in PP nanocomposites. Polymer. 2006;47:4638-48.
18. Varghese S, Karger-Kocsis J. Natural rubber-based nanocomposites by latex compounding with layered silicates. Polymer. 2003;44:4921-7.
19. Said M, Seif S, Challita G. Development of blown film linear low-density polyethylene-clay nanocomposites: part a: Manufacturing process and morphology. Journal of Applied Polymer Science. 2020;137:48589.

- **How to cite this article:** Zaman HU, Khan RA. Preparation and characterization of polypropylene/organo-muscovite clay nanocomposites by melt extrusion. Advanced Journal of Science and Engineering. 2022;3(1):23-34.
- https://doi.org/10.22034/advjse22031023